Single-File Diffusion of Neo-Pentane Confined in the MIL-47(V) Metal-Organic Framework

Aziz Ghoufi, Guillaume Maurin

Single-File Diffusion of Confined Neo-Pentane in the MIL-47(V) Metal-Organic Frameworks

A. Ghoufi *,† and G. Maurin ‡

†*Institut de Physique de Rennes, IPR, CNRS-Université de Rennes 1, UMR CNRS 6251, 35042 Rennes, France*

‡*Institut Charles Gerhardt Montpellier UMR 5253 CNRS UM Université Montpellier, Place E. Bataillon, 34095 Montpellier Cedex 05, France*

E-mail: aziz.ghoufi@univ-rennes1.fr

Abstract

Single-file diffusion of neo-pentane in the channel-like MIL-47(V) was recently revealed by Quasi Elastic Neutron Scattering experiments. The origin of such unprecedented dynamic behavior in the field of Metal-Organic Framework has not been elucidated at the atomistic level yet. Here molecular dynamics simulations are performed to first confirm the single-file diffusion of neo-pentane in MIL-47(V) and further unveil the molecular insights into this abnormal diffusion process and its connection with the flexibility of the framework. Whatever the loading, a sub-diffusive regime is highlighted, in good agreement with the single-file diffusion experimentally detected. We show that this sub-diffusive regime is un-correlated with the flexibility of the MIL-47(V) and comes mostly from the pore dimension of the MOF that hinders the crossing of molecules along the channel. Neither translation jumps nor correlation dynamics of the guest molecules present in the same channel and in the neighbors channels were observed. Moreover the rotational dynamics was also carefully explored and a relatively homogeneous rotational motion was evidenced along the three directions. While the translational diffusion coefficient decreases when the loading increases, the rotational diffusion coefficient remains constant which corresponds to a clear deviation to the Stokes Einstein relation.

Dedicated: The paper is dedicated to Dr. H. Jobic for his exceptional contribution in the experimental exploration of guest dynamics in MOFs and his invaluable support over the last 15 years.

Introduction

Owing to their high chemical versatility and their richness in terms of pore size/shape, a huge number of Metal-Organic Frameworks (MOF) architectures[1–5] has been reported so far, some of them showing promises in diverse applications including adsorption/separation,[6–13] energy storage,[14–18] catalysis,[19–21] nanomedecine[22] or nanofiltration.[23–25] This family of hybrid porous materials assembled by connecting a wide range of metal centers and a large diversity of organic linkers generating nanopores of different shapes (channels, cages, etc.) and sizes (from micropores to mesopores), are particularly attractive to capture gas molecules. Four physical processes control the adsorption/separation performances of MOFs, i) the adsorbed molecules/pore wall interactions, namely the thermodynamics (enthalpic)-effect, ii) the packing of the molecules most of the time assisted by the guest-responsive dynamics of the framework, iii) the molecular sieving where the pore aperture enables a full size exclusion of one molecule and iv) the kinetics/diffusion of the molecules into the pores. Whereas the three first criteria have been extensively examined both experimentally and theoretically, this is far to be the case for the diffusion[26–39] although many molecular separation exploit differences in transport properties.[40,41] Let us mention that the criteria (ii - packing) and (iii- sieving) are also influenced by the molecular mobility that emphasizes the need to assess the transport properties. Furthermore, from a more fundamental standpoint, it was demonstrated in some cases that molecules trapped in nanoporous materials can exhibit non-conventional diffusion behaviors related to their confinement at the nanoscale.[40,41]

During the past two decades, our computational strategy integrating force field Molecular Dynamics combined with Quasi-Elastic Neutron Scattering measurements (QENS) identified several dynamic behaviors of molecules confined in MOFs such as, the standard 1D or 3D diffusion in many small and large pore MOFs where the crossing of molecules such as hydrogen, methane and carbon dioxide is authorized.[29,30,36,39] These diffusion mechanisms are considered as "normal" from a Fickian point of view. Furthermore, this combination of experimental and computational approaches revealed a series of unusual diffusion behaviors including the supermobility of hydrogen and methane in

the 1D-channel MIL-53(Cr)[29,42] as well as the blowgun diffusion of linear alkanes[43] and the corkscrew dynamics of confined benzene both evidenced in the 1D-channel MIL-47(V).[44] Both MOFs are isostructural, built using metal oxide octahedral interconnected by 1,4-benzenedicarboxylate linkers, MIL-53(Cr) containing hydroxyl groups located at the metal-oxygen-metal links owing to the Cr oxidation state of +III while MIL-47(V) presents oxo bridges as the oxidation state of V is +IV (see Figure 1). More recently, an additional anomalous dynamics was evidenced experimentally by H. Jobic in MIL-47(V), namely a single-file diffusion of neo-pentane. This dynamics behavior is uncommon since it requires specific confinement conditions related to the ratio of the kinetic diameter of the molecules and the pore size to exclude mutual passages of the molecules along the channel, i.e. the molecules are confined to advancing one behind the other in the same direction. A single-file diffusion can be evidenced from the plot of the mean square displacement (MSD) for the guest as a function of time where MSD increases with $t^{0.5}$ contrary to the normal 1D diffusion where MSD increases with t. Indeed, this is the first evidence of such an unusual diffusion in the field of MOFs and only the second one in the field of porous materials. Indeed Jobic and coworkers reported in the past a single file diffusion process of methane in the pore of $AlPO_4$-5 material.[45] However, the origin of this unusual diffusion still remains unknown. In this work we aim to confirm this unusual diffusion phenomenon and further unveil the diffusion mechanism at the microscopic scale using molecular dynamics simulations implementing the flexibility of the MOF framework via the use of an appropriate force field.

Methods

Models and Computational Details

Neo-pentane was modeled by means of the uncharged united atoms (UA) TRAPPE force field which is able to reproduce accurately the thermodynamics properties of bulk phases[46] and the structure and the dynamics of confined alkanes.[49]In order to assess the impact of the force field for this guest, we also considered Optimized Potentials for

Liquid Simulations force fields (OPLS), i.e. the uncharged united-atoms (OPLS-UA)[47] and the charged all-atoms (OPLS-AA)[48] description. Additionally, the charges in the OPLS-AA model were re-calculated using a more sophisticated *ab*-initio calculation with the consideration of the 6-311g* basis set (OPLS-AA-CHG2). Details of charges calculation can be found elsewhere.[50]The MIL-47(V) framework was considered as flexible using the force field and partial charges we reported and validated in a previous study.[51] In order to evaluate the impact of the flexibility on the dynamics of neo-pentane, we also considered the MOF framework with the atoms fixed in their initial positions. Intermolecular interactions between neo-pentane and MIL-47(V) were modeled by combining electrostatic and van der Waals interactions. Electrostatic contribution was computed by using the Ewald sum with a convergence parameter of 0.36 $Å^{-1}$ while the van der Waals interactions were modeled by 12-6 Lennard Jones (LJ) potential. Crossed LJ interactions between MIL-47(V) and neo-pentane were evaluated from the Lorentz-Berthelot mixing rule with the consideration of a cutoff of 12 Å.

Initial configuration was built by considering the crystallographic data obtained from X-ray diffraction[51] and an orthorhombic large pore supercell of 240 unit cells (30x4x2) was constructed such as the initial cell lengths are L_z=55.756 Å, L_y=32.286 Å and L_x=409.08 Å. Neo-pentane molecules were thus randomly incorporated into the pore. Five loading were thus investigated, 0.25, 0.50, 0.75, 1.0 and 1.5 molecules per unit cell (molec./u.c.). An illustration of confined neo-pentane in the MIL-47(V) is given in Figure 1. All simulations were performed by using the DL_POLY code (version 4.0)[52] in the NσT statistical ensemble with N is the number of molecules, T is the temperature (300K) and σ is the anisotropic constraint (1 bar) to allow both size and shape of the MOF framework to vary. Canonical simulations (NVT, V is the volume) were also performed in the case of a rigid framework. Verlet-velocity propagator combined with the Nose-Hoover thermostat and barostat were considered.[53] Relaxation times of 0.5 ps for both thermostat and barostat were used. Acquisition phases were conducted during 10 ns with a time-step of 1 fs while the equilibration period was 2.5 ns.

Translational dynamics

Translational dynamics was assessed from the calculation of the mean square displacement (MSD) for neo-pentane defined as follows:

$$\mathrm{MSD}(t) = \frac{\left\langle \sum_{t_0} \sum_{i=1}^{N} \left[\mathbf{r}_{\mathrm{com},i}(t+t_0) - \mathbf{r}_{\mathrm{com},i}(t_0)\right]^2 \right\rangle}{NN_0 t} \tag{1}$$

with $\mathbf{r}_{\mathrm{com},i}$ the position of the center of mass of molecule i, t_0 the time origin, N the number of molecules and N_0 the number of t_0. We evidenced that the diffusion largely proceeds throughout the x axis corresponding to the direction of the channel such as

$$\mathrm{MSD}_x(t) = \frac{\left\langle \sum_{t_0} \sum_{i=1}^{N} \left[x_{\mathrm{com},i}(t+t_0) - x_{\mathrm{com},i}(t_0)\right]^2 \right\rangle}{NN_0 t} \sim \mathrm{MSD}(t) \tag{2}$$

From the MSD plot as a function of time and by using the generalized Einstein's relation, the diffusivity (D_f) can be extracted as follow

$$MSD(t) = AD_f t^{\alpha} \tag{3}$$

where A is a constant, α is a parameter related to the type of diffusion, $\alpha = 1$ corresponds to a diffusive regime, $\alpha < 1$ is connected to a sub-diffusive one while $\alpha > 1$ is linked to a super-diffusive process. The case of α=2 corresponds to a ballistic dynamics.[40,41,54] Let us mention, that for $\alpha \neq 1$, the diffusion is considered as anomalous. For a diffusive (Fickian) regime the diffusivity is related to the well-known self-diffusion coefficient (D_s) extracted from the Einstein's relation in one dimension ($MSD(t) = 2D_s t$). Here α was calculated by deriving Eq. 3 as

$$\alpha(t) = \frac{\partial MSD(t)}{\partial t} \cdot \frac{MSD(t)}{t} \tag{4}$$

For a pure single-file diffusion, the diffusivity corresponds to the single-file mobility factor (F) that can be defined as

$$MSD(t) = 2Ft^{0.5} \tag{5}$$

Rotational dynamics

The rotational dynamics can be examined by calculating the rotational diffusion coefficient (D_r) from a similar formalism that was employed for describing the translational dynamics. To do so, an orientational unit vector, corresponding to the dipole moment of the neo-pentane molecules was defined, $\tilde{\boldsymbol{\mu}}$. The cross product $\tilde{\boldsymbol{\mu}}(t) \wedge \tilde{\boldsymbol{\mu}}(t+\Delta t)$ gives the direction of the instantaneous axis of rotation for a vector rotational displacement $\Delta\varphi(t)$, whose magnitude is given by $\mid \Delta\varphi(t) \mid = \cos^{-1}(\tilde{\boldsymbol{\mu}}(t)\tilde{\boldsymbol{\mu}}(t+\Delta t))$. We can then define the total angular displacement by the following equation

$$\varphi(t) = \int_0^t \Delta\varphi(t^{'})dt^{'} \tag{6}$$

The Mean Square Angular Displacement (MSDA) is then provided by

$$MSDA(t) = \frac{\left\langle \left| \sum_{t_0} \sum_{i=1}^{N} \left[\varphi_i(t+t_0) - \varphi_i(t_0)\right]^2 \right| \right\rangle}{NN_0t} \tag{7}$$

$$MSDA(t) = D_r t^{\alpha} \tag{8}$$

$\alpha(t)$ and D_r were calculated using the same formalism that was employed for the translation dynamics (Eq. 3).

Results and Discussion

Figure 2 reports the MSD plots for neo-pentane at different loadings. For the five uptakes, the MSDs are not linear highlighting a non Fickian diffusion behavior of the guest molecules. The corresponding MSDs were fitted between 200 ps and $2 \cdot 10^3$ ps by using a power function (MSD=At^{α}). Indeed, between 0 and 200 ps the regime is rather ballistic whereas beyond $2 \cdot 10^3$ ps the diffusion is hindered due to the confinement environment generating the dynamical statistical noise. As shown in Figure 2, the MSDs for five neo-pentane uptakes are well fitted by the power function and the result i.e. the value of the exponent α is reported in Figure 3a. α is systematically smaller than 1 and this obser-

vation highlights a sub-diffusive regime in fair agreement with the recent experimental observation of the single-file diffusion of neo-pentane in this MOF (α=0.5).[55] α was also calculated from Eq. 4 between 200 ps and $2 \cdot 10^3$ ps and from $2 \cdot 10^3$ ps and $7 \cdot 10^3$ ps. Between 200 ps and $2 \cdot 10^3$ ps, Figure 3a shows that α is lower than 1.0 regardless the loading that is in line with the fitting procedure and it bears out the sub-diffusive regime. Let us mention that the fluctuations of α are due to the method of calculation based on the determination of a first derivative from a finite difference of 1st order. Regardless of the methods of calculation (fit and Eq. 4) and the considered time range, Figure 3a confirms a sub-diffusive regime for the confined neo-pentane into the MIL-47(V). By considering $\alpha = 0.5$ the diffusivity (or single-file mobility factor (F)) was evaluated by using Eq. 3 and represented as a function of the neo-pentane loading in Figure 3b. It shows that the single-file mobility factor decreases when the neo-pentane loading increases since the guest/guest interactions increase due to the reduction of the free volume available for the diffusion. This trend is similar to that of the self-diffusion coefficient of molecules confined in different environment.[43] Interestingly, the single-file mobility factor calculated from the simulated data at 0.25 molecule/u.c. by using the single-file model allowed us to obtain F=21.1 m^2 $ps^{-0.5}$ which is within the same range of value than the experimental data previously reported for a similar loading (F=8.0 $m^2ps^{-0.5}$ at 0.33 molecule/u.c.)[55]

Figure 2 also reports the MSD calculated from the experimental diffusivity by using a single-file diffusion model[55] for an uptake of 0.33 molecule/u.c.. The resulting MSD is depicted in Figure 2 , the resulting MSD is slightly lower than the simulated one. The deviation between QENS and MD simulations might be due to the force field used to represent neo-pentane. However Figure 4a shows that the MSD plots for neo-pentane modeled using the OPLS-UA, OPLS- AA, OPLS-AA-CHG2 and TRAPPE models are very similar that discards this assumption. Interestingly, the sub-diffusive regime is always captured regardless the atomistic model used for neo-pentane suggesting that the underlying physics is not force field dependent. Indeed the ultra-confinement prevails over the so-used force field. The deviation is most probably associated with the fact that

the calculated values of α is not exactly 0.5 as shown in Figure 3a.

Figure 4b further reports the MSD for neo-pentane calculated for a loading of 0.75 and 1.5 molecule/u.c. by considering a flexible and a rigid description of the MIL-47(V) framework. This figure clearly evidences that the flexibility of the MOF only weakly impacts the dynamics of the confined neo-pentane and its sub-diffusive dynamics leading to very similar simulated α values (Figure 4b) and simulated single-file mobility factor (Figure 3b) in both cases.

The diffusion mechanism of neo-pentane at the atomistic level was further revealed from the analysis of the 2D density calculated for the center of mass of the guest molecules in the pores of MIL-47(V) averaged over the MD trajectories. Typically Figures 5a and 5b report the 2D density distributions along both yx (direction along the channel) and zy (perpendicular to the channel) planes for a loading of 0.25 molecule/u.c.. These figures evidence that the guest molecules experience most of the space available in the channel, suggesting that the diffusion mechanism is not ruled by sequential translational jumps. Translational jumps can be also quantified by the calculation of the self Van Hove function $G_S(r,t)$) such as r and t are the position and time of guest molecules, respectively,

$$G_S(r,t) = \frac{1}{N}\left\langle \sum_{j=1}^{N} \delta\left[\mathbf{r} - (\mathbf{r}_j(t) - \mathbf{r}(0)\right] \right\rangle \quad (9)$$

where $r_j(t)$ is the atomic position of j particle at time t and N is the number of neo-pentane molecules. Figure 6a reports $G_S(r,t)$ from 1 ps to 14 ps for a loading of 0.25 molecule/u.c.. The maximum of the Van Hove function remains at a distance lower than 1.5 Å from 2 ps to 14 ps, which indicates small displacements and an absence of translational jumps in this time interval. To characterize the existence of the single-file diffusion defined by an absence of the crossing of molecules along the channel, we defined the variable $\Delta x(t) = x_i(t) - x_j(t)$ where x_i and x_j are the positions of two different i and j molecules along the x direction. Therefore, when $\Delta x(t) = 0$ both molecules i and j cross. Figure 6b which reports the distribution of Δx for both 0.25 and 1.5 molecules/u.c. shows that it is impossible to get $\Delta x = 0$. This suggests an absence of crossing molecules which is in line with a single-file process. The molecular process ruling the single file

diffusion corresponds to the impossibility of the molecules to interpass. This is related the ratio (kinetic diameter of the molecules/pore size) that excludes mutual passage. The number of neo-pentane clusters of different size was also calculated to examine an eventual packing of the molecules during the diffusion process. This calculation was performed by considering a separating distance of 6 Å between two molecules. This distance was selected from the position of the first peak of the radial distribution function between the center of mass of the corresponding guest molecules. These calculations led to 91% of single pentane molecules and only 9% of associated pairs. This clearly emphasizes the absence of a diffusion of packed molecules and supports that the molecules diffuse mostly as single molecules along the channel.

In the MIL-47(V) framework, center of two neighbors channels are separated by a distance of 13 Å and the inter-channels correlation might impact the diffusion mechanism of neo-pentane. To shed light on this possible correlation, MD simulations were performed with neo-pentane confined in a single long-channel typically for a loading of 0.25 molecule/u.c. (10 molecules in the channel) and compared to the simulations where all channels were randomly filled by 0.25 molecule/u.c.. The possible correlations have been evaluated from the calculation of the total structure factors as depicted in Ref.[56] Figure 7 reports very similar structure factors for both situations and this suggests the absence of correlations between the dynamics of neo-pentane molecules confined in two neighbors channels.

The rotational dynamics was also investigated and the MSDA for neo-pentane corresponding to a loading of 0.25 molecule/u.c. and 1.5 molecule/u.c. in the three x, y, and z directions as well as the total component are reported in Figure 8a. One observes that for both loadings, the MSDA are similar in all the directions. Indeed, the pore size is large enough along the y and z directions to avoid any hindering of the rotation of the molecules contrary to the translational dynamics where the translational degrees of freedom are frozen. Contrary to the translational diffusion component, the rotational dynamics shows a "normal" behavior given its time linear dependence. As exhibited in Figure 8b the rotational diffusion coefficient slightly fluctuates around 0.22 Rad.^{2}/ps

that corresponds to a relatively fast relaxation time of 13.4 ps. Interestingly, Figure 8b highlights a decorrelation between the translational and the rotational dynamics. Indeed, while F decreases with the loading, (D_r) is substantially constant. This observation is consistent with the evolution of the MSDA which remains similar for both 0.25 molecule/u.c. and 1.5 molecule/u.c loadings. This is the result of the loss of two translational degrees of freedom according to y and z given the high degree of confinement from a "translational" standpoint but not enough from a rotational one.

Concluding Remarks

In this work the dynamics of confined neo-pentane in the 1D-channel MIL-47(V) MOF was investigated by using Molecular Dynamics simulations with the consideration of a wide range of loading from 0.25 to 1.5 molecule/u.c. at 300 K. A single-file diffusion regime was simulated whatever the considered loading, thus confirming the experimental data previous reported by QENS measurements. A good agreement between the experimental and simulated single-file mobility factor was also obtained. We evidenced that this unusual diffusion behavior is un-correlated to the flexibility of the MIL- 47(V) and it is rather the result of the pore size effect that hinders the crossing of molecules in the channel. Moreover, from the calculated 2D-density plot for neo-pentane as well as the self Van Hove function and the structure factors we revealed the absence of translation jumps and the uncorrelated dynamics of neo-pentane between neighbors channels. Moreover, the diffusion was shown to mostly proceed via the mobility of single molecules rather than clusters. Eventually, we showed that while the translational diffusion decreases when the loading increases, the rotational diffusion coefficient remains constant which corresponds to a clear deviation to the Stokes Einstein relation. This work provides molecular insight into the nature of the gas transport in porous materials. This finding could be of great interest for the kinetic gases separation methods, gas storage and purification processes. It can contribute to a more basic understanding of the mechanisms that rule gas transport into porous catalysts, molecular sieves or nanofiltration through sub-nanoporous

biological and inorganic membranes.

Competing Financial Interest

The authors declare no competing financial interests.

Acknowledgements

We are grateful to the ANR for its financial support through the project "MEACOPA", ANR-17-CE29-0003.

References

(1) Hoskins, B.; Robson, R. Infinite polymeric frameworks consisting of three dimensionally linked rod-like segments. *J. Am. Chem. Soc.* **1989**, *111*, 5962-5964.

(2) Yaghi, O.; Li, H. Hydrothermal Synthesis of a Metal-Organic Framework Containing Large Rectangular Channels. *J. Am. Chem. Soc.* **1995**, *117*, 10401-10402.

(3) Kondo, M.; Yoshitomi, T.; Matsuzaka, H.; Kitagawa, S.; Seki, S. Three?Dimensional Framework with Channeling Cavities for Small Molecules: (M2(4, 4'-bpy)3(NO3)4.xH2O)n(M=Co,Ni,Zn). *Angew. Chem. Int. Ed. 36*, 1725-1727.

(4) Ferey, G. Hybrid porous solids: past, present, future. *Chem. Soc. Rev.* **2008**, *37*, 191-214.

(5) Maurin, G.; Serre, C.; Cooper, A.; Férey, G. The new age of MOFs and of their porous-related solids. *Chem. Soc. Rev.* **2017**, *46*, 3104-3107.

(6) Zhou, H.; Kitagawa, S. Metal-Organic Frameworks (MOFs). *Chem. Soc. Rev.* **2014**, *43*, 5415-5418.

(7) Hamon, L.; Llewellyn, P. L.; Devic, T.; Ghoufi, A.; Clet, G.; Guillerm, V.; Pirngruber, G. D.; Maurin, G.; Serre, C.; Driver, G. et al. Co-adsorption and separation of CO2-CH4 mixtures in the highly flexible MIL-53(Cr) MOF. *J. Am. Chem. Soc.* **2009**, *131*, 17490-17499.

(8) Schröder, M. *Functional Metal-Organic Frameworks: Gas storage, Separation and Catalysis*; Springer Science & Business Media, 2010.

(9) Yu, C.-H.; Huang, C.-H.; Tan, C.-S. A Review of CO_2 Capture by Absorption and Adsorption. *Aerosol an Air Quality Research* **2012**, *12*, 745-769.

(10) Bon, V.; Kavoosi, N.; Senkovska, I.; Kaskel, S. Tolerance of Flexible MOFs toward Repeated Adsorption Stress. *ACS Appl. Mater. & Interfaces* **2015**, *7*, 22292-22300.

(11) Adil, K.; Belmabkhout, Y.; Pillai, R. S.; Cadiau, A.; Bhatt, P.; Assen, A.; Maurin, G.; Eddaoudi, M. Gas/vapour separation using ultra-microporous metal–organic frameworks: insights into the structure/separation relationship. *Chem. Soc. Rev.* **2017**, *46*, 3402-3430.

(12) Cadiau, A.; Belmabkhout, Y.; Adil, K.; Bhatt, P.; Pillai, R.; Shkurenko, A.; Martineau-Corcos, C.; Maurin, G.; Eddaoudi, M. Hydrolytically stable fluorinated metal-organic frameworks for energy-efficient dehydration. *Science* **2017**, *356*, 731-735.

(13) Belmabkhout, Y.; Bhatt, P.; Adil, K.; Pillai, R. S.; Cadiau, A.; Shkurenko, A.; Maurin, G.; Liu, G.; Koros, W. J.; Eddaoudi, M. Natural gas upgrading using a fluorinated MOF with tuned H2S and CO2 adsorption selectivity. *Nat. Energy* **2018**, *3*, 1059-1066.

(14) Getman, R.; Bae, Y.; Wilmer, C.; Snurr, R. Review and analysis of molecular simulations of methane, hydrogen, and acetylene storage in metal-organic frameworks. *Chem. Rev.* **2012**, *112*, 703-723.

(15) Makal, T.; Li, J.-R.; Lu, W.; Zhou, H.-C. Methane storage in advanced porous materials. *Chem. Soc. Rev.* **2012**, *43*, 7761-7779 .

(16) Arico, A.-S.; Bruce, P.; Scrosati, B.; Tarascon, J.-M.; Schalkwijik, W. V. Nanostructured materials for advanced energy conversion and storage devices. *Nat. Mater.* **2005**, *4*, 366-377.

(17) Jiang, J.; Furukawa, H.; Zhang, Y. B.; Yaghi, O. M. High Methane Storage Working Capacity in Metal–Organic Frameworks with Acrylate Links. *J. Am. Chem. Soc.* **2016**, *138*, 10244-10251.

(18) Suh, M.; Park, H.; Prasad, T.; Lim, D. Hydrogen storage in metal-organic frameworks. *Chem. Rev.* **2012**, *112*, 782-835.

(19) Doonan, C.; Sumby, C. Metal-organic framework catalysis. *CrysEngComm* **2017**, *19*, 4044-4048.

(20) Zhu, L.; Liu, X.-Q.; Jiang, H.-L.; Sun, L.-B. Metal-Organic Frameworks for Heterogenous Basic Catalysis. *Chem. Rev.* **2017**, *117*, 8129-8176.

(21) Rogge, S.; Bavykina, A.; Hajek, J.; Garcia, H.; Olivos-Suarez, A.; Sepulveda-Escribano, A.; Vimont, A.; Clet, G.; Bazin, P.; Kapteijin, F. et al. Metal–organic and covalent organic frameworks as single-site catalysts. *Chem. Soc. Rev.* **2017**, *46*, 3134-3184 .

(22) Horcajada, P.; Baati, G.; Allan, P.; Maurin, G.; Couvreur, P.; Férey, G.; Morris, R.; Serre, C. Metal organic framework in biomedicine. *Chem. Rev.* **2012**, *112*, 1232-1268.

(23) Campbell, J.; Burgal, J. S.; Szekely, G.; Davies, R.; Braddock, D.; Livingston, A. Hybrid polymer/MOF membranes for Organic Solvent Nanofiltration (OSN): Chemical modfication and the quest for perfection. *J. Mem. Sci.* **2016**, *503*, 166-176.

(24) Yang, F.; Efome, J.; Rana, D.; Matsuura, T.; Lan, C. Metal-Organic Frameworks Supported on Nanofiber for Desalination by Direct Contact Membrane Distillation. *ACS Appl. Mater. & Interfaces* **2018**, *10*, 11251-11260.

(25) Zhang, H.; Hou, J.; Hu, Y.; Wang, P.; Ou, R.; Jiang, L.; Liu, J. Z.; Freeman, B.; Hill, A.; Wang, H. Ultrafast selective transport of alkali metal ions in metal organic frameworks with subnanometer pores. *Sci. Adv.* **2018**, *4*, 0066-0074.

(26) Skoulidas, A.; Sholl, D. Self-diffusion and transport diffusion of light gases in metal organic framework materials assessed using molecular dynamics simulations. *J. Phys. Chem. BChem. B* **2005**, *109*, 15760-15768.

(27) Amirjalayer, S.; Tafipolsky, M.; Schmid, R. Molecular dynamics simulation of benzene diffusion in MOF-5: importance of lattice dynamics. *Angew. Chem. Int. Ed.* **2007**, *46*, 463-466.

(28) Greathouse, A.; Allendorf, M. Force field validation for molecular dynamics simulations of IRMOF-1 and other isoreticular zinc carboxylate coordination polymers. *J. Phys. Chem. C.* **2008**, *112*, 5795-5802.

(29) Rosenbach, N.; jobic, H.; Ghoufi, A.; anf G. Maurin, F. S.; Bourrelly, S.; Llewellyn, P.; Devic, T.; Serre, C.; Ferey, G. Quasi-elastic neutron scattering and molecular dynamics study of methane diffusion in metal organic frameworks MIL-47(V) and MIL-53(Cr). *Angew. Chem. Int. Ed.* **2008**, *47*, 6611-6615.

(30) Salles, F.; Kolokolov, D.; Jobic, H.; Maurin, G.; Llewellyn, P.; Devic, T.; Serre, C.; Férey, G. Adsorption and Diffusion of H-2 in the MOF Type Systems MIL-47(V) and MIL-53(Cr): A Combination of Microcalorimetry and QENS Experiments with Molecular Simulations. *J. Phys. Chem. C* **2009**, *113*, 7802-7812.

(31) Salles, F.; Jobic, H.; Llewellyn, P.; Serre, C.; Bourrelly, S.; Férey, G.; Maurin, G. Transport diffusivity of CO2 in the Highly Flexible Metal-Organic Franmework MIL-53(Cr). *Angew. Chem. Int. Ed.* **2009**, *48*, 8335-8339.

(32) Seehamart, K.; Nanok, T.; Krishna, R.; Baten, J. V.; Remsungnen, T.; Fritzsche, S. A Molecular Dynamics investigation of the influence of framework flexibility on self-diffusivity of ethane in Zn(tbip) frameworks. *Microporous Mesoporous Mater.* **2010**, *125*, 97-100.

(33) Haldoupis, E.; Watanabe, T.; Nair, S.; Sholl, D. Quantifying large effects of framework flexibility on diffusion in MOFs: CH4 and CO2 in ZIF-8. *ChemPhysChem* **2012**, *3*, 3449-3452.

(34) Nugent, P.; Belmabkout, Y.; Burd, S.; Cairns, A.; Luekbe, R.; Forest, K.; Pham, T.; Ma, S.; Space, B.; Wojtas, L. et al. Porous materials with optimal adsorption thermodynamics and kinetics for CO2 separation. *Nature* **2013**, *495*, 80-84.

(35) Garcia-Pérez, E.; Serra-Crespo, P.; Hamad, S.; Kapteijn, F.; Gascon, J. Molecular simulation of gas adsorption and diffusion in a breathing MOF using a rigid force field. *Phys. Chem. Chem. Phys.* **2014**, *16*, 16060-16066.

(36) Rosenbach, N.; Jobic, H.; Ghoufi, A.; Devic, T.; Koza, M.; Ramsahye, N.; Mota, C.; Serre, C.; Maurin, G. Diffusion of Light Hydrocarbons in the Flexible MIL-53(Cr) Metal-Organic Framework: A Combination of Quasi-Elastic Neutron Scattering Experiments and Molecular Dynamics Simulations. *J. Phys. Chem. C* **2014**, *118*, 14471-14477.

(37) Verploegh, R.; Nair, S.; Sholl, D. Temperature and loading-dependent diffusion of light hydrocarbons in ZIF-8 as predicted through fully flexible molecular simulations. *J. Am. Chem. Soc.* **2015**, *137*, 15760-15771.

(38) Prakash, M.; Jobic, H.; Ramsahte, N.; Nouar, F.; Borges, D.; Serre, C.; Maurin, G. Diffusion of H-2, CO2, and Their Mixtures in the Porous Zirconium Based Metal Organic Framework MIL-140A(Zr): Combination of Quasi-Elastic Neutron Scattering Measurements and Molecular Dynamics Simulations. *J. Phys. Chem. C* **2015**, *119*, 23978-23989.

(39) Kolokolov, D.; Jobic, H.; Rives, S.; Yot, P.; Olivier, J.; Trens, P.; Stepanov, A.; Maurin, G. Diffusion of Benzene in the Breathing Metal-Organic Framework MIL-53(Cr): A Joint Experimental-Computational Investigation. *J. Phys. Chem. C* **2015**, *119*, 8217-8225.

(40) Berrod, Q.; Hanot, S.; Guillermo, A.; Mossa, S.; Lyonnard, S. Water sub-diffusion in membranes for fuel cells. *Scientific Reports* **2017**, *7*, 8326-8340.

(41) Flenner, E.; Das, J.; Rheninstadter, M.; Kosztin, I. Subdiffusion and lateral diffusion coefficient of lipid atoms and molecules in phospholipid bilayers. *Phys. Rev. E* **2009**, *79*, 011907-011919.

(42) Salles, F.; Jobic, H.; Maurin, G.; Koza, M.; Llewellyn, P.; Devic, T.; Serre, C.; Ferey, G. Experimental Evidence Supported by Simulations of a Very High H2 Diffusion in Metal Organic Framework Materials. *Phys. Rev. Lett.* **2008**, *100*, 245901-245906.

(43) Jobic, H.; Rosenbach, N.; Ghoufi, A.; Kolokolov, D.; Yot, P.; Devic, T.; Serre, C.; Ferey, G.; Maurin, G. Unusual Chain Length Dependence of n-Alkanes diffusion in the Metal Organic Framework MIL-47(V) : the Blowgun effect. *Chem. - A European Journal* **2010**, *16*, 10337-10341.

(44) Kolokolov, D. I.; Jobic, H.; Stepanov, A.; Olivier, J.; Rives, S.; Maurin, G.; Devis, T.; Serre, C.; Férey, G. Experimental and Simulation Evidence of a Corkscrew Motion for Benzene in the Metal−Organic Framework MIL−47. *J. Phys. Chem. C* **2012**, *116*, 15093-15098.

(45) Jobic, H.; Hahn, K.; Karger, J.; bée, M.; Tuel, A.; Noack, M.; Girnus, I.; Kearley, G. Unidirectional and Single-File Diffusion of Molecules in One-Dimensional Channel Systems. A Quasi-Elastic Neutron Scattering Study. *J. Phys. Chem. C* **1997**, *101*, 5834–5841.

(46) Martin, M.; Siepmann, J. Novel configurational-bias Monte Carlo method for branched molecules. Transferable potentials for phase equilibria. 2. United-atom description of branched alkanes. *J. Phys. Chem. B* **1999**, *103*, 4508-4517.

(47) Jorgensen, W.; Madura, J.; Swenson, C. Optimized intermolecular potential functions for liquid hydrocarbons. *J. Am. Chem. Soc.* **1984**, *106*, 6638-6646.

(48) Jorgensen, W.; Maxwell, D.; Tirado-Rives, J. Development and Testing of the OPLS All-Atom Force Field on Conformational Energetics and Properties of Organic Liquids. *J. Am. Chem. Soc.* **1996**, *118*, 11225-11236.

(49) Santos, M.; Franco, L.; Castier, M.; Economou, I. Molecular dynamics simulation of n-alkanes and CO2 confined by calcite nanopores. *Energy&fuels* **2018**, *32*, 1934-1941.

(50) Ghoufi, A.; Deschamps, J.; Maurin, G. Theoretical Hydrogen Cryostorage in Doped MIL-101(Cr) Metal-Organic Frameworks. *J. Phys. Chem. C* **2012**, *116*, 10504-10509.

(51) Yot, P.; ma, Q.; Haines, J.; Yang, Q.; Ghoufi, A.; Devic, T.; Serre, C.; Dimitriev, V.; Férey, G.; Zhong, C. et al. Large breathing of the MOF MIL-47(VIV) under mechanical pressure: a joint experimental–modelling exploration. *Chem. Sci.* **2012**, *3*, 1100-1104.

(52) Todorov, I.; Smith, W.; Trachenko, K.; Dove, M. DLPOLY3: new dimensions in molecular dynamis simulations via massive parallelism. *J. Mater. Chem.* **2006**, *16*, 1911-1918.

(53) Hoover, W. Canonical dynamics: Equilibrium phase-space distributions. *Phys. Rev. A* **1985**, *31*, 1695-1697.

(54) Bouchaud, J.-P.; Georges, A. Anomalous diffusion in disordered media: Statistical Mechanisms, Models and Physical Applications. *Physics Reports* **1990**, *195*, 127-293.

(55) Jobic, H. Observation of single-file diffusion in a MOF. *Phys. Chem. Chem. Phys* **2016**, *18*, 17190-17195.

(56) Ghoufi, A.; Hureau, I.; Morineau, D.; Renou, R.; Szymczyk, A. Confinement of tert-Butanol Nanoclusters in Hydrophilic and Hydrophobic Silica Nanopores. *J. Phys. Chem. C* **2013**, *117*, 15203-15212.

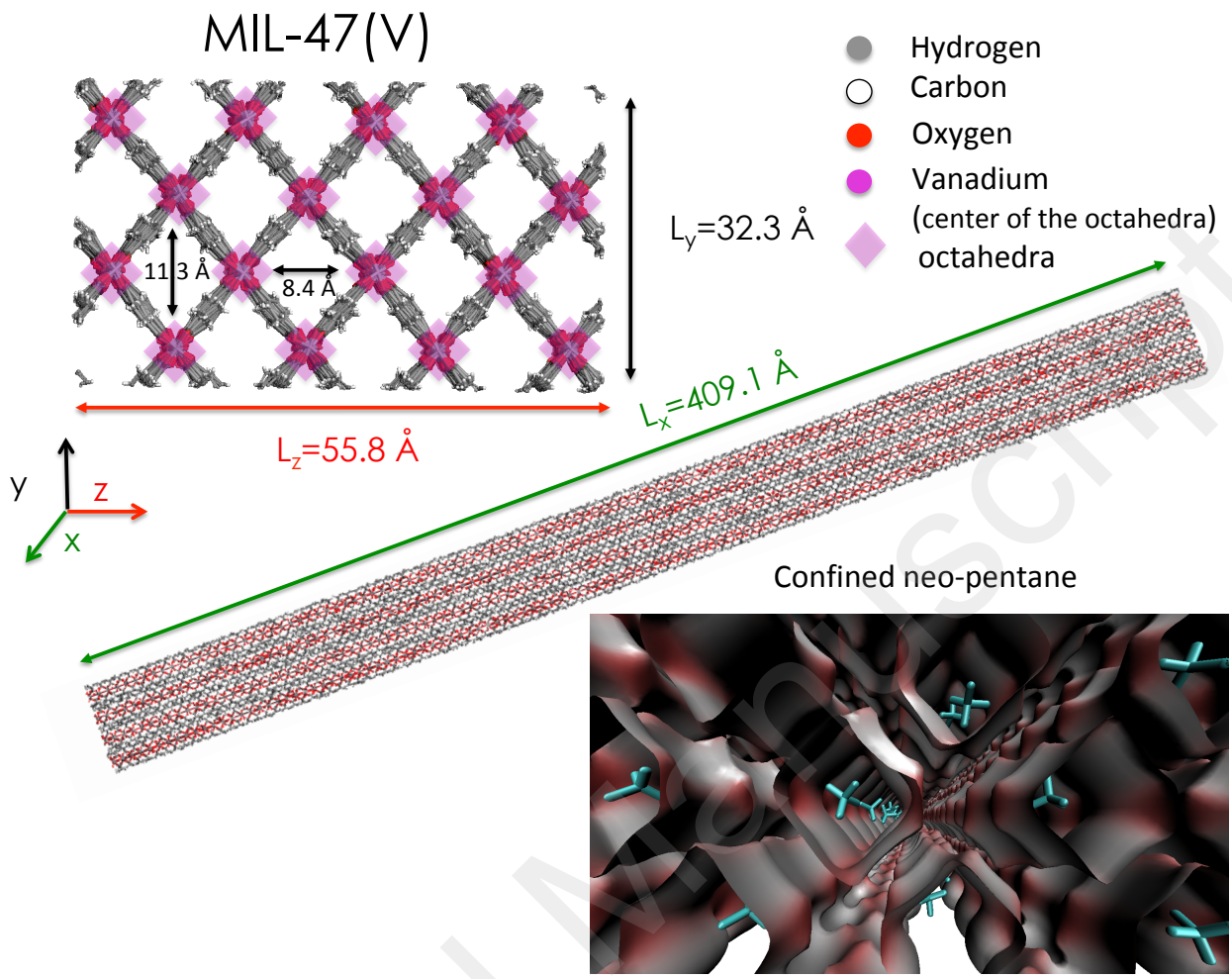

Figure 1 Illustration of the MIL-47(V) MOF material and the confined neo-pentane (in cyan color) molecules into the 1D channel. The box lengths according to x(L_x), y(L_y) and z(L_z) directions are also indicated. The MIL-47 (V) material is represented from the Connolly surface to illustrate the confined neo-pentane.

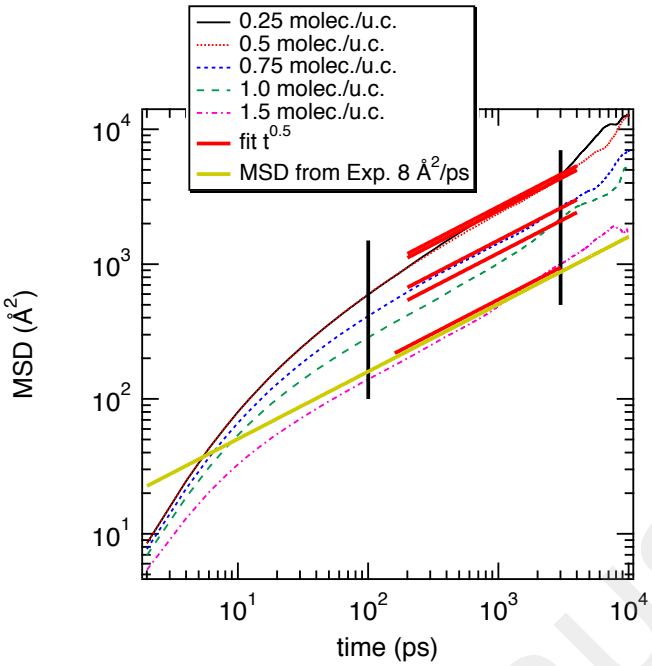

Figure 2 Mean square displacements for the center of mass of neo-pentane calculated for the five different loadings at 300 K.

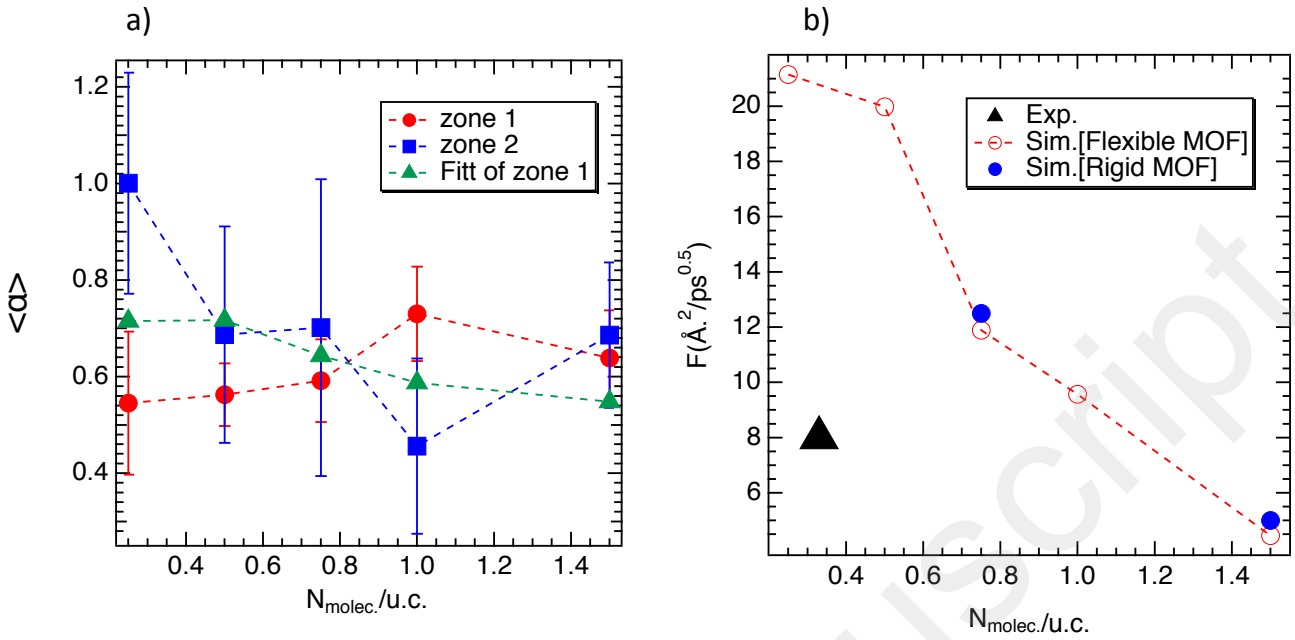

Figure 3 a) Exponent α calculated from Eq. 4 in two time regions, zone 1: between 200 ps and $2 \cdot 10^3$ ps ps and zone 2: between $2 \cdot 10^3$ ps and $7 \cdot 10^3$ ps; and from a fitting procedure using a power function, plotted as a function of the neo-pentane loading. b) Evolution of the single-file mobility factor as a function of the neo-pentane loading.

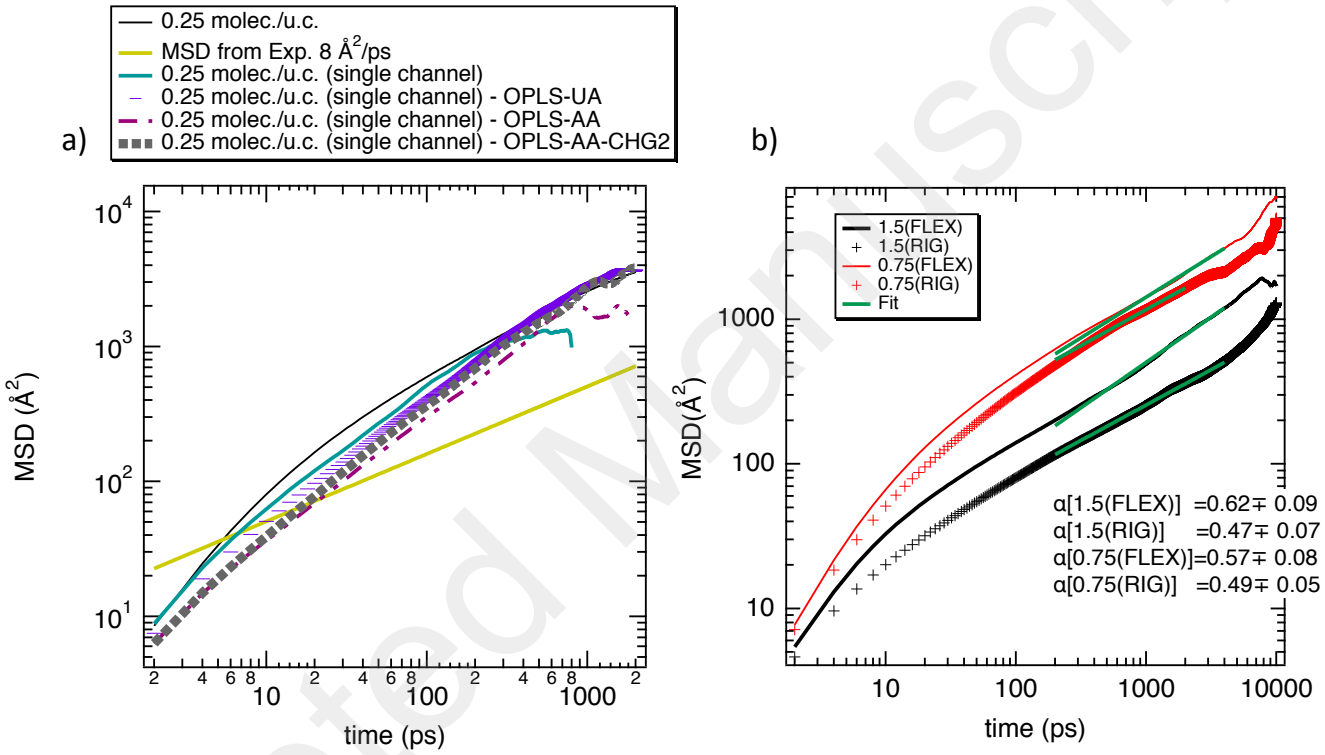

Figure 4 a) Mean square displacement for the center of mass of neo-pentane calculated for a loading of 0.25 molecule/u.c. and different force fields to represent neo-pentane. b) Mean square displacement for the center of mass of neo-pentane calculated for two loadings at 0.75 and 1.5 molecule/u.c using both flexible and rigid frameworks. Exponents α were calculated from Eq. 4 between 200 ps and $2 \cdot 10^3$ ps. The fit using a power function is also represented.

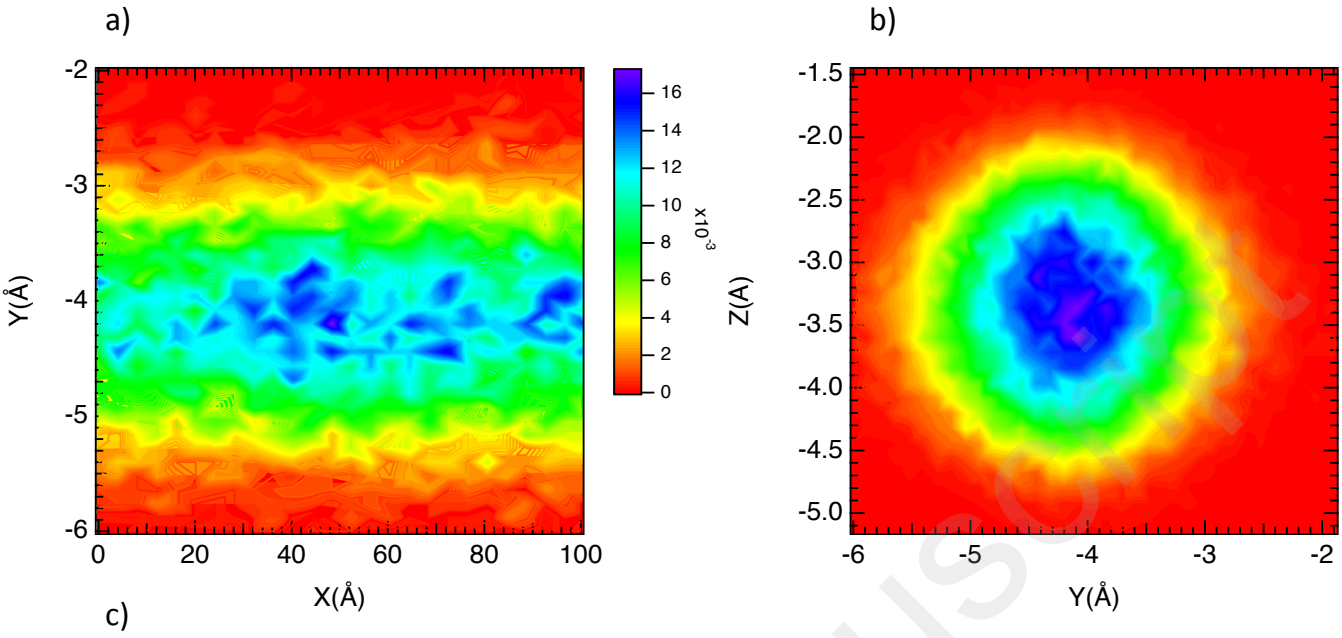

Figure 5 2D density distribution for neo-pentane plotted along (a) yx direction along the channel of the MIL-47(V) and (b) zy direction perpendicular to the channel of the MIL-47(V) calculated for a loading of 0.25 molecule/u.c.

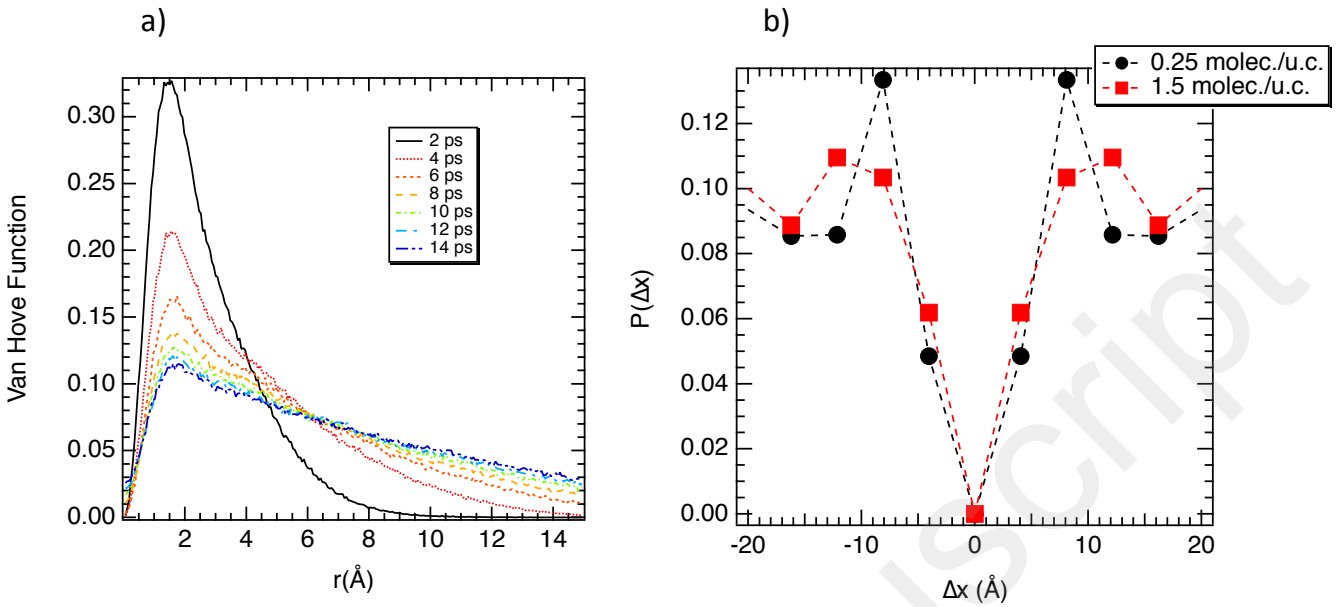

Figure 6 a) Self van Hove function calculated as a function of the covered distance for characteristic times for a loading of 0.25 molecule/u.c. b) Probability distribution of Δx for two loadings.

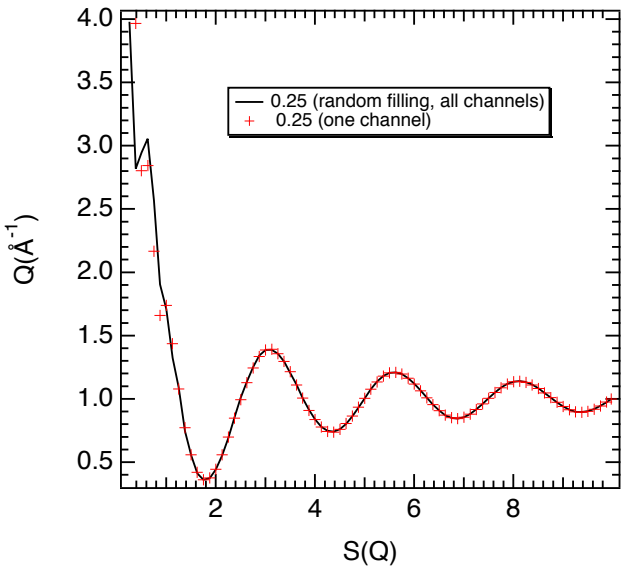

Figure 7 Total structure factor of confined neo-pentane in the MIL-47(V) for a loading of 0.25 molecule/u.c. for two distinct simulations i) a random filling in all channels for a loading of 0.25 molecule/u.c. and ii) loading in a single channel for a loading of 0.25 molecule/u.c. i.e. 10 molecules in the channel.

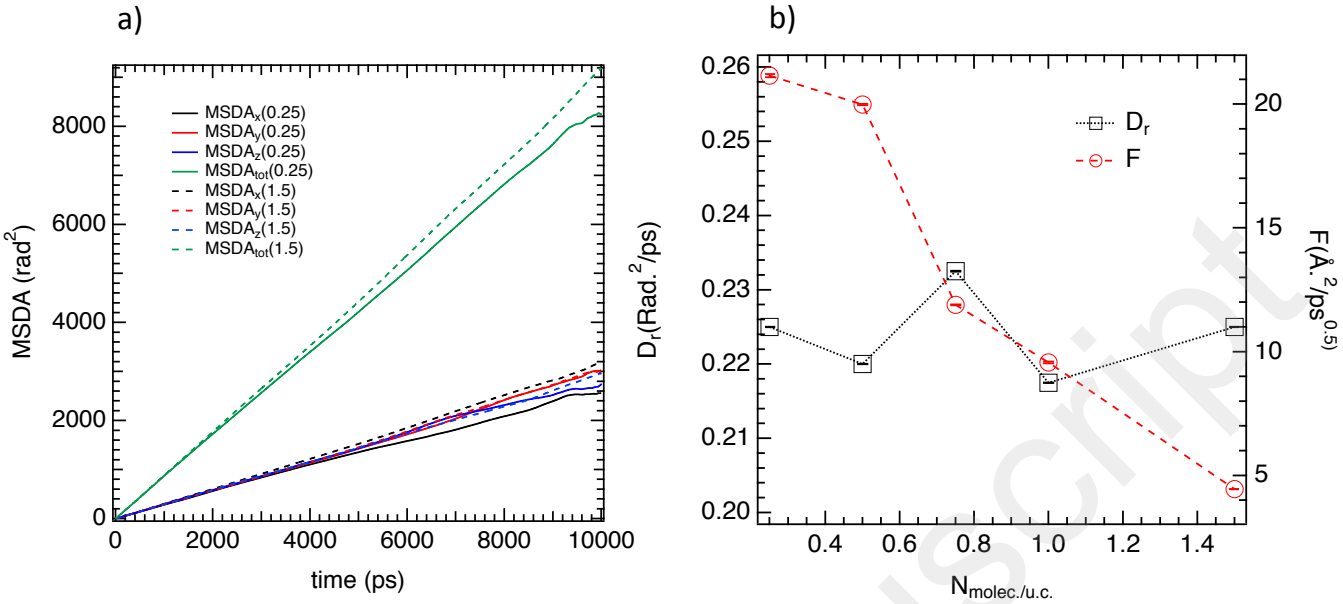

Figure 8 a) x, y, z and total contributions of MSDA as a function of time for the loading of 0.25 and 1.5 molecule/u.c. b) rotational diffusivity (left axis) and single-file mobility factor (right axis) as a function of the loading.

Graphical TOC Entry